

Spectral analysis of waveguide tapered microfiber with an ultrathin metal coating

Cheng-Ling Lee

*Department of Electro-Optical Engineering and Optoelectronics Research Center, National United University,
No. 1 Lien-Da, Kung-Ching Li, Miaoli 360, Taiwan
cherry@nuu.edu.tw*

Abstract: This work demonstrates the feasibility of a novel dispersion engineered ultrathin metal film coated on a tapered fiber with a thickness of around 10nm. To our knowledge, the dispersion characteristics of the proposed device induced by such an extremely thin metal film are described here for the first time. Experimental and simulation results indicate that the metal thin film has unique dispersion properties and intrinsic optical characteristics of strong absorption and high reflection in the near infrared light of a wavelength range of 1.25~1.65 μm , making the material and waveguide dispersions of tapered-fibers more tailorable. In addition to the ability to flatten the slope of the fundamental-mode cutoff of the transmission spectrum, the dispersion profile is heavily influenced when the ultrathin metal film is coated around the proposed tapered fibers. The optical characteristics of the spectral response caused by the ultrathin film on tapered microfibers are also investigated and analyzed.

©2010 Optical Society of America

OCIS codes: (060.2340) Fiber optics components; (310.6860) Thin films, optical properties; (230.7370) Waveguides; (230.7408) Wavelength filtering devices.

References and links

1. F. A. Burton, and S. A. Cassidy, "A complete description of the dispersion relation for thin metal film plasmon-polaritons," *J. Lightwave Technol.* **8**(12), 1843–1849 (1990).
2. A. Diez, M. V. Andres, and J. L. Cruz, "In-line fiber-optic sensors based on the excitation of surface plasma modes in metal-coated tapered fibers," *Sens. Actuators B Chem.* **73**(2-3), 95–99 (2001).
3. A. Diez, M. V. Andres, D. O. Culverhouse, and T. A. Birks, "Cylindrical metal-coated optical fibre devices for filters and sensors," *Electron. Lett.* **32**(15), 1390–1392 (1996).
4. J. M. Corres, F. J. Arregui, and I. R. Matias, "Sensitivity optimization of tapered optical fiber humidity sensors by means of tuning the thickness of nanostructured sensitive coatings," *Sens. Actuators B Chem.* **122**(2), 442–449 (2007).
5. R. K. Verma, A. K. Sharma, and B. D. Gupta, "Modeling of Tapered Fiber-Optic Surface Plasmon Resonance Sensor With Enhanced Sensitivity," *IEEE Photon. Technol. Lett.* **19**(22), 1786–1788 (2007).
6. R. Jha, R. K. Verma, and B. D. Gupta, "Surface Plasmon Resonance-Based Tapered Fiber Optic Sensor: Sensitivity Enhancement by Introducing a Teflon Layer between Core and Metal Layer," *Plasmonics* **3**(4), 151–156 (2008).
7. B. Li, Y. Liu, Z. Tan, H. Wei, Y. Wang, W. Ren, and S. Jian, "Using of non-uniform stress effect to realize the tunable dispersion of the fiber Bragg grating with tapered metal coatings," *Opt. Commun.* **281**(6), 1492–1499 (2008).
8. A. Diez, M. V. Andres, and J. L. Cruz, "Hybrid surface plasma modes in circular metal-coated tapered fibers," *J. Opt. Soc. Am. A* **16**(12), 2978–2982 (1999).
9. R. Slavik, J. Homola, J. Ctyroky, and E. Brynd, "Novel spectral fiber optic sensor based on surface plasmon resonance," *Sens. Actuators B Chem.* **74**(1-3), 106–111 (2001).
10. G. B. Smith, and A. I. Maarouf, "Optical response in nanostructured thin metal films with dielectric over-layers," *Opt. Commun.* **242**(4-6), 383–392 (2004).
11. A. Diez, M. V. Andres, and D. O. Culverhouse, "In-Line Polarizers and Filters Made of Metal-Coated Tapered Fibers: Resonant Excitation of Hybrid Plasma Modes," *IEEE Photon. Technol. Lett.* **10**(6), 833–835 (1998).

12. R. Slavik, J. Homola, and J. Ctyroky, "Single-mode optical fiber surface plasmon resonance sensor," *Sens. Actuators B Chem.* **54**(1-2), 74–79 (1999).
 13. M. Piliarik, J. Homola, Z. Manikova, and J. Ctyroky, "Surface plasmon resonance sensor based on a single-mode polarization-maintaining optical fiber," *Sens. Actuators B Chem.* **90**(1-3), 236–242 (2003).
 14. R. Willsch, "High performance metal-clad fiber-optic polarisers," *Electron. Lett.* **26**(15), 1113–1115 (1990).
 15. R. Scarmozzino, and R. M. Osgood, Jr., "Comparison of finite-difference and Fourier-transform solutions of the parabolic wave equation with emphasis on integrated-optics applications," *J. Opt. Soc. Am. A* **8**(5), 724–731 (1991).
 16. P. N. Moar, S. T. Huntington, J. Katsifolis, L. W. Cahill, A. Roberts, and K. A. Nugent, "Fabrication, modeling, and direct evanescent field measurement of tapered optical fiber sensors," *J. Appl. Phys.* **85**(7), 3395–3398 (1999).
 17. H. A. Macleod, *Thin Film Optical Filters*, 3rd Ed., Institute of Physics Publishing, (Bristol and Philadelphia, 2001), Chap. 2 and Chap.4.
 18. K. Okamoto, *Fundamentals of Optical Waveguides* (Academic, 2006), Chap. 3.
 19. <http://refractiveindex.info>
 20. S.-Y. Chou, K.-C. Hsu, N.-K. Chen, S.-K. Liaw, Y.-S. Chih, Y. Lai, and S. Chi, "Analysis of Thermo-Optic Tunable Dispersion-Engineered Short-Wavelength-Pass Tapered-Fiber Filters," *J. Lightwave Technol.* **27**(13), 2208–2215 (2009).
-

1. Introduction

Metal coating on micro-fiber devices has received considerable interest for technology applications. However, related research topics focus mainly on surface plasmon resonance (SPR) of the metal thin film in device applications. Such SPR-based devices have been extensively adopted to excite surface plasmon-polaritons wave for use as high extinction ratio polarizers and many highly sensitive sensors [1–14]. The metal material has a dielectric constant with a large negative real part and a small imaginary part, which is equivalent to having a complex refractive index ($n-ik$) of a smaller refractive index (n) and a significantly larger extinction coefficient (k), which has a high reflection and high absorption feature. Therefore, the optical characteristic of the metal material may uniquely differ from dielectric materials due to the opposite sign of the dielectric constant. Restated, although most dielectric materials are transparent over a wide spectral range and can always be manufactured for integrated fiber components, they are unavailable for nano-scale integrated applications owing to the inability to solve the diffraction-limited problem. To our knowledge, this work describes for the first time the optical characteristics and qualitative analysis of fundamental-mode cutoff (FMC) with an ultrathin thickness of around 10nm, with a metal film coated around the tapered fibers. This work also analyzes the dispersion characteristics of an ultrathin metal film on tapered fibers since the waveguide and material dispersions significantly influence the optical properties of FMC. Dispersion control is of priority concern for many micro-fiber components in different applications. The dispersion can normally be engineered and tailored locally by modifying the waveguide structure or the constituting material of tapered-fiber to achieve novel fiber passive and active devices. Particularly, waveguide dispersion (WD) can be engineered and tailored by using a rearrangement of the waveguide structure, similar to multilayer cladding, nano-wire structure, or a photonic crystal structure. Therefore, owing to a small n , large k and significant dispersive characteristics of the ultrathin metal film, the dispersion property can be characterized when the unique ultrathin metal film is coated around the waveguide. This work demonstrates the feasibility of a novel dispersion-engineered method on an ultra-thin metal-coated tapered micro-fiber (UTMCTMF) device. The numerical results are calculated by the finite difference beam propagation method (FD-BPM) [15,16] to analyze and compare those results with the experimental ones. Importantly, an ultra-thin Al film can form a special cutoff spectral response of FMC to be flattened over a broader wavelength range when the matched index liquid surrounds the device. Moreover, owing to the high reflectivity of a metal film, the higher-order mode short wavelengths might be well-confined to propagate in the fiber in order to create a novel filter for photonic device

applications. Experimental and simulation results demonstrate the feasibility of such a novel micro device in facilitating the implementation of a highly effective dispersion engineering method for micro-fiber component applications.

2. Experiment and Simulation

Tapered fiber was fabricated by a SMF-28 single mode fiber, in which the core and cladding are $8.2\ \mu\text{m}$ and $125\ \mu\text{m}$ in diameter, respectively, ($D_{\text{co}}\sim 8.2\ \mu\text{m}$, $D_{\text{cl}}\sim 125\ \mu\text{m}$) which was pulled and heated under autocontrol by LabVIEW with tapered equipment. This work focused on manufacturing a tapered fiber with an extremely uniform waist diameter and smoother tapered transitions length (τ), with the desired tapered length (L) and shape. Following tapering of the fiber until the diameter (D) of $D = 30\ \mu\text{m}$, aluminum (Al) ultrathin film was then coated around the surface of the tapered fiber with a thickness of around $d = 10\ \text{nm}$ by high vacuum evaporation with a deposition rate of $5\ \text{\AA}/\text{sec}$. The thickness and deposition rate of the thin film were monitored by STM-100/MF Thickness/Rate Monitor with $1\ \text{\AA}$ thickness resolution. There are many advantages to use Al metal in this study, they include: easy to evaporate and always has good reflection in the infrared region, further with an additional advantage of adhering strongly to most substances. Furthermore, when compare with other metal materials, like Au (gold) and Ag (silver), Al has a vantage not generating the SPR efficiently since the main goal of the presented paper is to study the spectral transmission responses and cutoff characteristics of fundamental-mode field on the devices. There is an unattractive feature that it may form a thin and hard Aluminum oxide layer with about $1\sim 2\ \text{nm}$ on the $10\sim 20\ \text{nm}$ Al films' surface very quickly after coating [17]. Aluminum oxide film is a very low absorption dielectric material in wavelength range $300\ \text{nm}\sim 5\ \mu\text{m}$ and the thickness of Aluminum oxide is extremely thin which can be treated as a portion of the surrounding medium. Therefore we ignored the effect caused by the Aluminum oxide layer in the simulation work.

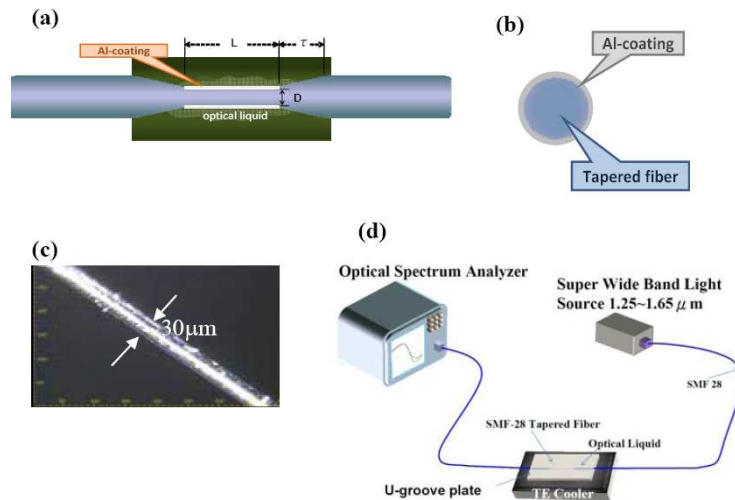


Fig. 1. (a) Diagram of the proposed Al-coated tapered optical fiber structure. (b) Cross section of the device. (c) Side view of the uniform waist of Al-coated tapered fiber with a good shine of metal gloss by the $1000\times$ CCD camera. (d) Experimental setup used to measure the transmission spectra of the proposed devices.

Figure 1(a) schematically depicts the proposed ultra-thin metal-coated tapered micro-fiber (UTMCTMF) filter, which is immersed in Cargille[®] index-matching optical liquid with an interaction length of the Al thin film coated uniform section. Figure 1(b) displays the cross section of the device, while Fig. 1(c) shows the side-view of the device. According to this

figure, good shine of metal luster can be observed due to the Al thin film coated around the device. Figure 1(d) shows the experimental setup for measuring the UTMCTMF. The transmission spectra are evaluated using the optical spectrum analyzer (OSA) with use of a Wide Band Light Source (WBL) in a wavelength range of 1.25~1.65 μm (spectral power density $> -26\text{dBm/nm}$) while transmitting the tapered fiber immersed in Cargille[®] liquid with a temperature controlled by TE cooler at 25°C. In addition to more closely examining the optical characteristics of the proposed UTMCTMF filters, this work also compares those results with the experimental results by theoretically calculating the optical transmission spectra, fundamental-mode cutoff (FMC) phenomena, propagation constant (effective index) and propagation performance of an optical wave through the UTMCTMF devices based on use of the numerical finite difference beam propagation method (FD-BPM) [15,16]. The following paragraph defines and describes the parameters and conditions in the simulation study.

The cutoff condition occurs when the normalized propagation constant b for fundamental-mode approaches zero, in which b is defined by the following equation [18]:

$$b = \frac{n_{\text{eff}}^2 - n_s^2}{n_c^2 - n_s^2} \quad (1)$$

where n_{eff} represents complex the effective index of a fundamental-mode for the proposed device that can be defined as $n_{\text{eff}} = n_{\text{eff}}^R - in_{\text{eff}}^I$, n_c and n_s are refractive indices of the new core of the tapered fiber and surrounding medium, respectively. This observation allows us to define FMC wavelength as the wavelength when $n_{\text{eff}} \rightarrow n_s$ appears. Figure 2 schematically depicts the fundamental-mode field propagating in the waveguide taper. The fundamental mode in the uniform taper waist stretches through Al film and extends to the outer material. Electromagnetic wave propagating through an absorbing media can generally be expressed as [17]:

$$E = E_0 \exp(-\alpha L) \cdot \exp(i(\omega t - \beta L)) \quad (2)$$

where E_0 denotes maximal amplitude of the mode field. Also, α attenuation coefficient which is defined as $\alpha = \omega \cdot n_{\text{eff}}^I / c$, n_{eff}^I can be regarded as decay rate that depends on extinction coefficient of the metal; L refers to the propagating length, ω the angular frequency, λ wavelength, and c represents the velocity of light in free space, β propagation constant is expressed as $\beta = (2\pi/\lambda) \cdot n_{\text{eff}}^R$, and t represents the propagation time of the wave. Figure 3 shows the following refractive indices of the material dispersion profiles of original core: n_{co} , silica cladding: n_{cl} for the SMF-28 tapered fiber, optical liquid Cargille[®] index liquids with $n_{\text{D}} = 1.456, 1.455, 1.454,$ and 1.452 and the coated metal material, aluminum (Al) used in the simulation. According to Fig. 3(b), refractive index (n) and extinction coefficient (k) of metal Al become increasingly large when the wavelength shifts to longer wavelength region revealing a high reflection and high absorption of optical characteristics. The material refractive index slopes are positive, which are opposite and different from the optical dielectric materials with negative slopes, as shown in Figs. 3(a) and 3(b) [19].

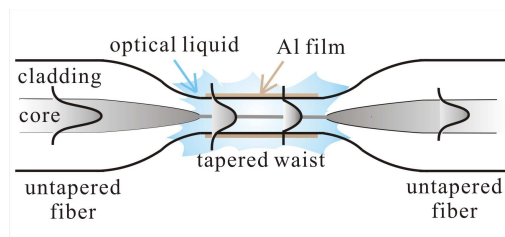


Fig. 2. Schematic diagram of mode field propagation in the tapered core that stretches through Al film and extends to the outer material in the tapered waist.

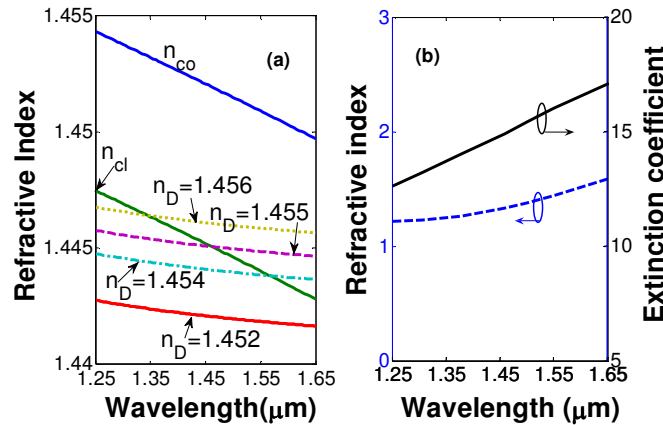


Fig. 3. Refractive index dispersion profiles for the (a) SMF-28 tapered fiber and optical liquid Cargille® index liquids, (b) metal material, aluminum: Al used in the simulation.

3. Results and discussion

This work has attempted to more thoroughly understand the fundamental-mode cutoff (FMC) characteristics of the proposed devices by performing experiments and simulations for comparison. Exactly how different ultrathin metal films affects tapered fibers is studied by fixing the transition length of $\tau = 6\text{mm}$ in the experimental and simulated cases. The ultrathin layer determined here is from the view point of geometrical structure for the optical waveguide. The thickness of few tens of nanometers (nm) for the metal film is extremely thin when compare with $30\mu\text{m}$ waist of the presented tapers. Moreover, one can also see Fig. 7 in the Ref. [20], the wavelength $1.25\sim 1.35\mu\text{m}$ light in the waist of $30\mu\text{m}$ taper shows the fundamental mode field diameter is about $40\sim 50\mu\text{m}$ which are also much greater than the size of metal thin film used in this study. Figure 4(a) shows experimental (dashed lines), simulated (solid lines) spectral transmission, of which, red and blue lines represent non-coated and 10nm -coated of the devices, respectively. According to this figure, the tapered fiber with an Al thickness of around 10 nm shows a short-pass cutoff with a flatter slope than the sharpest slope of the non-coated when using an index liquid of $n_D = 1.456$. This is owing to that the Al film has a high reflectance at near infrared wavelengths so that the cutoff wavelengths become less leaky. This figure also reveals around a 2dB loss for the non-coated tapered fiber and around 5dB for the coated device in practical measurements when compared with those of theoretical simulation results. Simulated and experimental results seem to be agreements in the cutoff wavelengths and the curves of the optical spectra. According to the above results, the FMC slightly shifts to a shorter wavelength when the filter is coated around Al film,

whereas the slope of FMC flattens after coating. This finding suggests that propagation constant (effective index) and propagation performance of electric or magnetic field of the optical wave are influenced and changed when the structural changes of the waveguide by coating such an ultrathin metal film. As for the intrinsic property for a negative dielectric constant of the metal, the proposed filter possesses a lower effective index, higher absorption loss in the transmission region (short wavelengths), flatter slope in the transition region and higher reflection in the attenuation region (long wavelengths) than those of a non-coated device. Figure 4(b) shows the diagram that defines the transmission, transition and attenuation regions in the optical spectra of the filter. The attenuation region is defined the spectral range which is under -30dB transmission. Above results demonstrate that the dispersion characteristics of waveguide can be engineered by the ultrathin metal film, which can strongly vary cutoff wavelengths and spectral response for such devices.

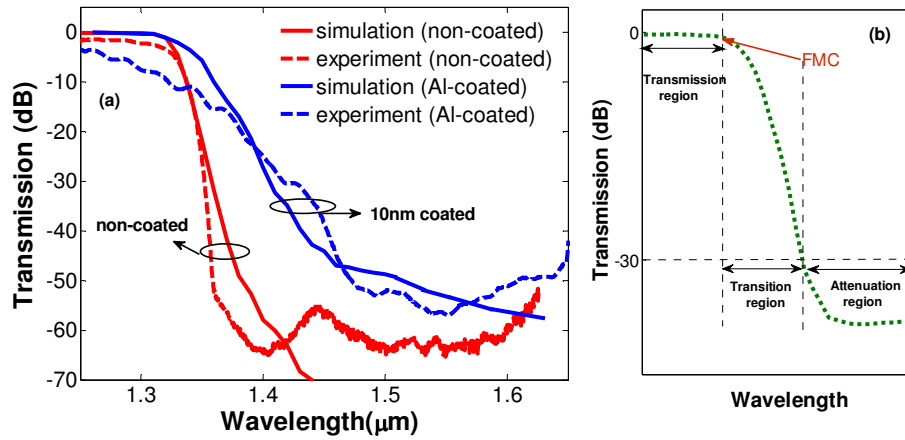


Fig. 4. (a) Experimental and simulated transmission spectra of uniform tapered waist $D = 30\mu\text{m}$ with non-coated (red lines) and Al-coated UTMCTMF of 10nm (blue lines), (b) Diagram of cutoff, transmission, transition and attenuation wavelength regions of optical spectra.

Owing to that the Al film is ultrathin, the evanescent field can penetrate through the film to reach the outer surrounding liquid but suffers from absorption in the metal thin film layer. According to Fig. 5(a), the tapered fiber without Al coating produces a clear short-pass steep cutoff, whereas a thicker Al film can flatten the cutoff curve in the transition region. Moreover, transmission profiles with further loss in the transmission region and are less leaky in the attenuation region when the metal film thickness increases. Those properties are attributed to that the evanescent fields of propagated guided waves (shorter wavelengths) are lossy in the metal layer; however, non-guided waves (longer wavelengths) can be partly reflected by the metal layer. Obviously, reflectance in the attenuation region can be reduced with a decreasing thickness of the metal film; a thinner metal film is thus expected to produce a steeper short-pass cutoff than that of the thicker film. Figures 5(b) and 5(c) show the effective indices and dispersion profiles in transmission region of the UTMCTMF for fundamental modes. The dispersion parameter (ps/nm/km) of the waveguide can be estimated by the following Eq. (3) [17]:

$$D = -\frac{\lambda}{c} \frac{d^2 n_{eff}}{d\lambda^2} \quad (3)$$

where n_{eff} is only considered the real part of the effective index owing to that the calculated value of the imaginary part n_{eff}^I is extremely small with the order of $10^{-6} \sim 10^{-7}$. Once the index liquid $n_D = 1.456$ is used, short-pass cutoff wavelengths occur around $1.3 \sim 1.322 \mu\text{m}$ when the coated thickness ranges from 200nm to 0nm (non-coated). According to Fig. 5(b), the effective index of the fundamental mode crosses the refractive index lines of the surrounding medium at cutoff conditions and cannot guide the light in the proposed device any more above the cutoff wavelengths and besides the FMC shifts to a shorter wavelength with an increasing thickness. Additionally, the attenuation for the stopband becomes larger since the metal film is reduced to make the evanescent field extend outside the metal more, subsequently leading to higher losses, as shown in Fig. 5(a). In Fig. 5(c), dispersion ripples in the transmission region becomes increasingly higher on average when the metal film thickness increases, owing to that the absolute slope of material dispersion for the metal film is larger than those of silica based materials.

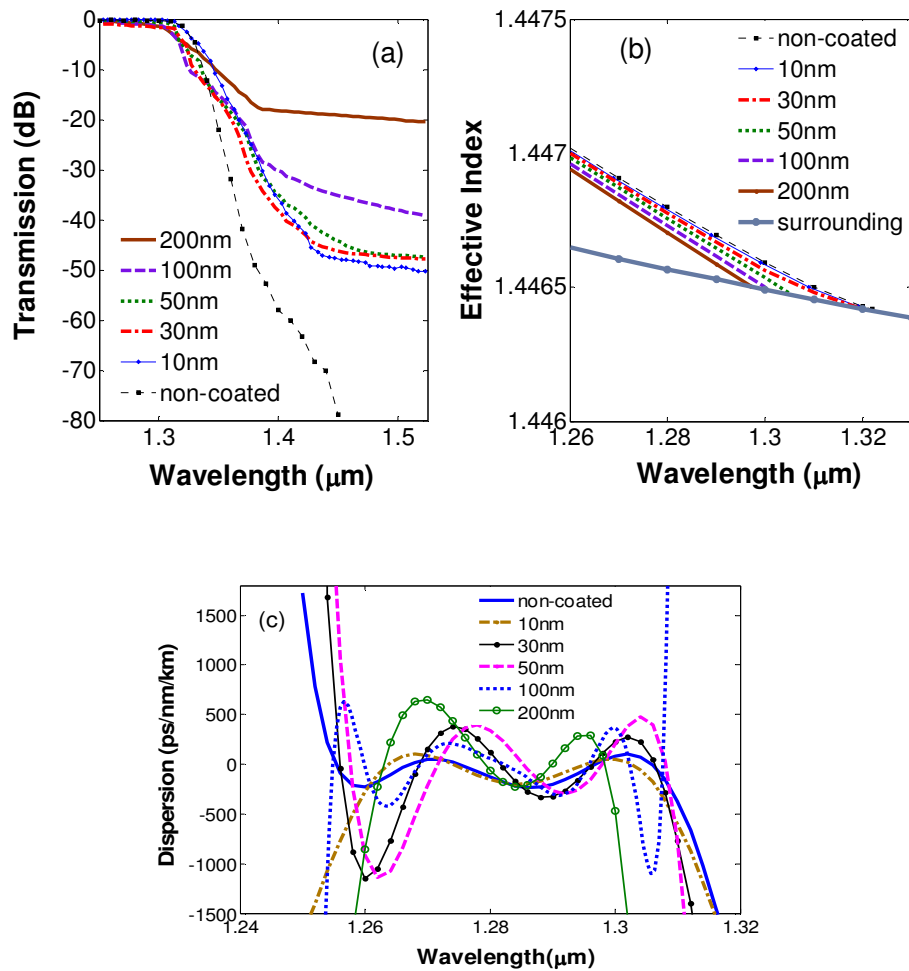


Fig. 5. Simulation results of (a) transmission spectra, (b) effective indices, and (c) dispersion profiles of fundamental-mode in the UTMCTMF at different Al-coated thicknesses with a thin film length of $L = 1.5\text{cm}$, where the Cargille® optical liquid is $n_D = 1.456$.

It is worth to mention that the transmission spectra in Fig. 5(a) seem to be very similar on the cases of thickness from 10 to 50nm because the thicknesses are so ultrathin and contributing the similar effects on the spectral response. On the other hand, the cutoff transmission spectra appear distortion and different if thickness greater than 100nm since fundamental-mode field suffered more absorption loss in transmission region and higher reflection in attenuation region. One can see again from the results of Fig. 5(b), the corresponding cutoff wavelengths are different for the cases of thickness 10, 30, and 50nm which are about 1.3207 μm , 1.3160 μm and 1.3051 μm , respectively. That means the cutoff slopes in transition region are slightly getting flat when thickness increases. Despite the slightly different cutoff slopes, the transmission spectra are very similar on the cases of thickness from 10 to 50nm. Therefore, we can classify these thicknesses as the ultrathin layers for the proposed UTMCTMF devices since the thickness are very thin when compare with the dimension of the mode fields with several tens micrometers.

When the uniform-waist section is immersed in different Cargille[®] index-matching liquids, the optical properties, especially cutoff wavelengths of the UTMCTMF, can be sensitively tuned as well. Therefore, a highly sensitive sensor can also be achieved by using such devices. According to Fig. 6(a), the cutoff wavelengths of the transmission spectra substantially shift to longer wavelengths when the refractive index of the liquid is slightly reduced. The tuning sensitivity of around 100nm shift corresponds to a refractive index variation of 0.001. Obviously, no FMC occurs over a wideband when the liquid $n_D = 1.452$ is used (dotted-dashed line in Fig. 6). We can see again the simulation results in Fig. 6(a), the transmission spectra having cutoff responses can be observed when the Cargille[®] optical liquids with $n_D = 1.456\sim 1.454$ are used. Figure 6(b) shows the effective index of the proposed filters with $d = 10\text{nm}$ and $D = 30\mu\text{m}$ and refractive indices of various surrounding media.

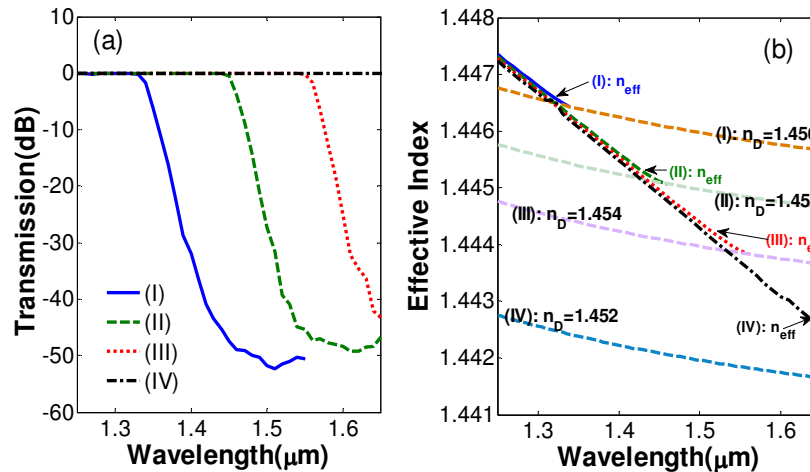


Fig. 6. Simulation results of (a) transmission spectra and (b) effective indices of the fundamental mode for UTMCTMF filters when using different Cargille index liquids.

Figure 7 also displays the FMC of transmission spectra of the devices at different Al-metal lengths of $L = 0.5\text{cm}$, 1.5cm and 3.0cm , respectively, with $n_D = 1.456$, $d = 10\text{nm}$ and $D = 30\mu\text{m}$. According to this figure, the attenuation for stopband becomes larger when the metal-coated thin film lengthens since the evanescent field extends outside and propagates through longer length of a metal film, leading to higher losses while the FMC wavelengths are almost the same of the three samples. Moreover, the waveguide dispersion behaviors with different

tapered waist diameters of the UTMCTMF devices with Al thin film of 10nm can explain the FMC of spectral characteristics in Fig. 8. The band-edge shifts to longer wavelengths as the waist diameter increases and slopes of FMC curves flatten with more loss in the attenuation band when the waist size is smaller. This phenomenon can also be demonstrated by the fundamental-mode field distribution from the literature [20]. If the diameter of non-coated tapered fiber $\leq 30\mu\text{m}$ (the cladding size), the fundamental-mode field is greatly extended into the surrounding region and subjected to a smoother cutoff slope. Especially with a size $< 10\mu\text{m}$, the spectral response of the fundamental mode incurs a strong loss in the transmission region and the cutoff slope flattens much more. However, in the presented UTMCTMF filters, the spectral responses are nearly the same in the transition and attenuation regions when diameters are below $30\mu\text{m}$ due to the reflection phenomenon since the fundamental-mode field significantly spreads out and experiences the metal film directly. Even with diameters less than $10\mu\text{m}$, the loss in the transmission region is significantly lower than with those in the non-coated tapered filters reported in the above mentioned paper [20].

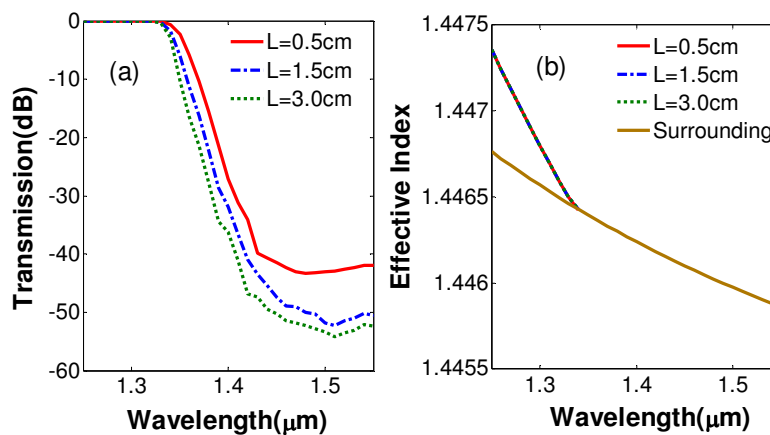


Fig. 7. Simulation results of (a) transmission spectra and (b) effective indices of the fundamental mode for the UTMCTMF filters with Al film of 10nm at different lengths of Al thin film 0.5cm, 1.5cm and 3.0cm.

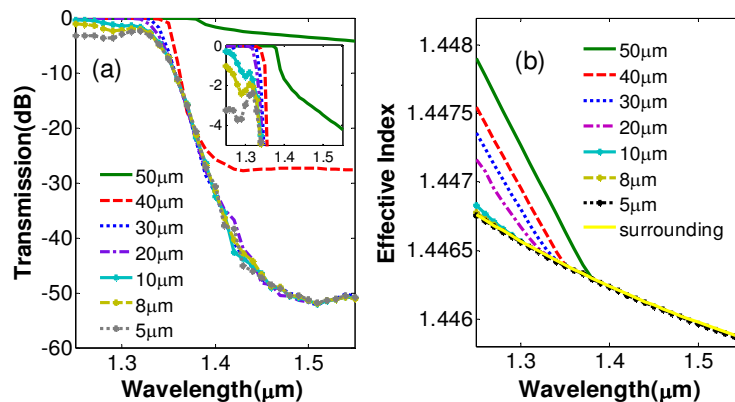


Fig. 8. Simulation results of (a) transmission spectra and (b) effective indices of the fundamental mode for the UTMCTMF filters with Al film of 10nm at different waist diameters.

It is worth to know, according to Fig. 8(b), the effective indices of the devices with waist diameters below $10\mu\text{m}$ are nearly close to the refractive index of surrounding liquid, which incur a large loss in the transmission region. However, almost the same spectral profiles in transition and attenuation regions due to the reflection by the metal film, as shown in Fig. 8(a). Above results demonstrate that the ultrathin thickness of 10nm has a significant waveguide dispersion engineered effect on the tapered microfiber.

4. Conclusions

This work has demonstrated and analyzed the feasibility of dispersion engineered method on the filters of ultra-thin metal-coated tapered microfiber (UTMCTMF). The ultrathin metal thin film with a negative dielectric constant and positive material dispersion slope for refractive index (n) and extinction coefficient (k) reduces the effective index and variation of waveguide dispersion as well as the optical cutoff characteristics of spectral response for the tapered microfiber. Therefore, in contrast with dielectric materials, the metals can make the material and waveguide dispersions of the tapered-microfibers more tailored due to their intrinsic optical characteristics of strong absorption and high reflection. Experimental verification and theoretical analyses are also performed. The results further demonstrate that the slopes of the FMC can be flattened in the transition region, with additional loss incurred in the transmission region, and less leaky in the attenuation region in the resulting spectral responses of the presented devices. Analysis results of the proposed devices significantly contribute to a novel dispersion engineered and practical applications, thus facilitating the development of new photonic components for sensing and telecommunication applications.

Acknowledgment

The author thanks Prof. Nan-Kuang Chen of Department of Electro-Optical Engineering and Optoelectronics Research Center, National United University for providing the tapered fiber samples. This research is supported by the National Science Council of the Republic of China, NSC 97-2221-E-239-012 and NSC 98-2221-E-239-002-MY2.